Quantum-mechanical calculation of H on Ni(001) using a model potential based on first-principles calculations

Mattsson, T.R.; Wahnström, G.; Bengtsson, L.; Hammer, Bjørk

Published in:
Physical Review B

Link to article, DOI:
10.1103/PhysRevB.56.2258

Publication date:
1997

Document Version
Publisher's PDF, also known as Version of record

Quantum-mechanical calculation of H on Ni(001) using a model potential based on first-principles calculations

Thomas R. Mattsson,* Göran Wahnström,† and Lennart Bengtsson‡
Department of Applied Physics, Chalmers University of Technology and University of Göteborg, S-412 96 Göteborg, Sweden

Bjørk Hammer§
National Center for Supercomputing Applications (NCSA), University of Illinois at Urbana-Champaign, Urbana, Illinois 61801 and Center for Atomic-Scale Materials Physics and Department of Physics, Technical University of Denmark, DK-2800 Lyngby, Denmark

(Received 10 October 1996)

First-principles density-functional calculations of hydrogen adsorption on the Ni (001) surface have been performed in order to get a better understanding of adsorption and diffusion of hydrogen on metal surfaces. We find good agreement with experiments for the adsorption energy, binding distance, and barrier height for diffusion at room temperature. A model potential is fitted to the first-principles data points using the simulated annealing technique and the hydrogen band structure is derived by solving the three-dimensional Schrödinger equation. We find vibrational excitation energies slightly too high, with about 10%, compared with experiments and very narrow hydrogen bands. The experimentally observed absence of a pronounced isotope effect for hydrogen diffusion at low temperatures is discussed in terms of tunneling in a static three-dimensional potential. [S0163-1829(97)05124-2]

I. INTRODUCTION

Hydrogen adsorption on metal surfaces has become a model problem for studying chemisorption and diffusion.

One of the more frequently studied systems is H on Ni(001). We are particularly interested in the diffusion process, especially at low temperatures where quantum effects are important. Both experimentally[1–3] and theoretically[4–8] a distinct change of the temperature dependence of the diffusion constant has been found when lowering the temperature; from an activated Arrhenius behavior at high temperatures to a nearly temperature-independent diffusion at low temperatures. The interpretation of the latter is that the diffusion process is dominated by tunneling between localized ground states for the hydrogen atom. The experimentally determined magnitude for the diffusion constant at low temperatures does not show any strong isotope dependence,[1,3] which provides a challenge for theoretical treatments.[9,10]

To get a good description and understanding of the diffusion process accurate models for the interatomic interactions are required. Several different model potentials have been proposed for the H/Ni(001) system,[7,8,11–14] but a common feature for most of these potentials is that they are fitted to experimentally determined parameters which mostly reflect properties of the equilibrium configuration. When dealing with diffusion and tunneling, however, not only the equilibrium configuration is important but also properties along the diffusion and tunneling paths. The development of electron-structure calculations using the density-functional theory has been rapid during the last years[15] and it has now become feasible to obtain quite high accuracy for a variety of systems including H interacting with metal surfaces.[16] This opens the possibility of calculations from first-principles properties of the potential-energy surface which are crucial for the details of the diffusion process. We have therefore performed total-energy calculations for H on Ni(001) using the density-functional theory, pseudopotentials, and plane-wave expansions for the electronic wave functions. The results are presented in Sec. II.

The first-principle calculation of the total energy is time consuming and one can only afford such calculations for a limited number of configurations. In the present paper we also determine the vibrational frequencies and the tunneling matrix element for hydrogen and thus the total energy for many points are required. We have therefore interpolated between the first-principles data points using a model potential for the interatomic interaction. The details of the fitting procedure are given in Sec. III and the resulting model potential is found to reproduce quite well the data points from the first-principles calculations.

In Sec. IV the model potential is used to evaluate the vibrational excitation energies and the corresponding bandwidths by solving the Schrödinger equation for hydrogen on a numerical grid. The vibrational frequencies are found to compare well with the experimental data.

The calculated values for the bandwidths are used in Sec. V to discuss the isotope dependence of the tunneling diffusion rate. If the curvature of the potential perpendicular to the tunneling path increases when moving from the center to the bridge position the isotope effect will be less pronounced compared with the usual square root dependence in the Wentzel-Kramers-Brillouin (WKB) exponent due to the zero-point motion effect. If this effect is large that could explain at least a part of the absence of a pronounced isotope effect at low temperatures, without invoking motion of the lattice atoms. Using the present first-principles data for the total energy we can now determine the magnitude of this effect. We find that the curvature around the bridge position is indeed larger compared with the equilibrium (center) position but the change is not sufficiently large to explain the experimental results. In a forthcoming study[17] the effect of lattice motion will be investigated.

II. FIRST-PRINCIPLES CALCULATIONS

The first-principles calculations are based on the density-functional theory with the full atomic potential for hydrogen and the pseudopotential by Troullier and Martins[18] for the nickel atoms. The wave functions are expanded in plane waves with an energy cutoff of 50 Ry and are self-consistent in the local-density approximation (LDA). The generalized gradient approximation (GGA-II) (Ref. 19) correction is then calculated using the LDA densities. The energies are extrapolated to zero fictitious electronic temperature (T_{el}) from the value $k_B T_{el}=0.1$ eV, used in the calculations. The full Brillouin zone is sampled with 100 k points which gives 15–25 in the irreducible zone depending on the position of the hydrogen atom. The Kohn-Sham equations are solved by means of the conjugate gradients method[15] and the self-consistent occupation numbers are found via a minimization of the electronic energy.[20]

We study a slab with five nickel layers with a monolayer of hydrogen on one side of the slab and vacuum on the other side. The size of the vacuum region is 10.4 Å. We use the LDA lattice constant for Ni (3.47 Å) and we allow the metal atoms to relax in the perpendicular direction (001) in presence of the adsorbed hydrogen. The distance between the first and second layer increases with 0.12 Å and between the second and third layer the increase is 0.10 Å. The relaxation of the clean metal surface on the opposite side of the slab is inwards and smaller; the first layer relaxes 1.7% inwards relative to the fixed middle layer. The most important relaxation is accounted for since the remaining forces on the metal atoms are of the order of ten times less than the corresponding forces for a truncated bulk slab with adsorbed hydrogen at the equilibrium position. In all subsequent calculations the nickel atoms will be kept fixed in these relaxed positions.

Only the perpendicular relaxation can be accounted for since the calculations are done for a monolayer coverage. This is a limitation since other relaxations can influence the behavior. In a forthcoming study[17] the relaxation for both hydrogen and deuterium, treated fully quantum mechanically using the present model potential, will be discussed. The desirable combination of first-principles calculations of energies and forces and a quantum-mechanical description of hydrogen is still, for computational reasons, out of reach, and we must resort to model potentials for quantum-mechanical calculations.

The total energy has been determined for different heights of the adsorbed hydrogen atom at four different locations on the surface, shown in Fig. 1. These different positions cover the most important regions of the surface for hydrogen vibration, diffusion, and tunneling. In Fig. 2 we show the results for the total energy together with the model potential developed in the next section. The zero of the energy scale is determined from the calculated adsorption energy, which we define as the difference between the energy with hydrogen adsorbed $E_{H,Ni}$ and the sum of the energy for a single hydrogen atom E_H and the energy for the bare nickel slab E_{Ni}:

$$E_{ads}=E_{H,Ni}-(E_H+E_{Ni}). \quad (1)$$

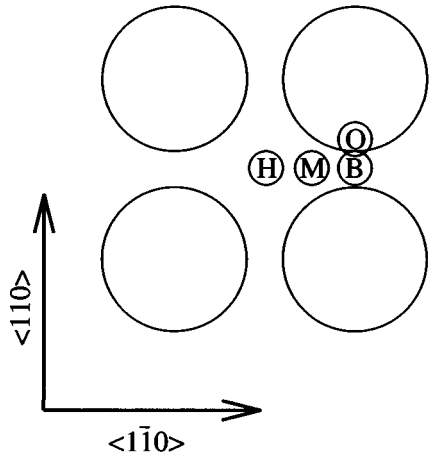

FIG. 1. The four points indicate where the first-principles calculations have been performed on the (001) surface. H: hollow site; B: bridge site; M: midsite, half-way between the hollow and bridge sites; O: off site, 0.15 Å away from the bridge site and perpendicular to the H-M-B path.

E_{ads} is thus the depth of the potential well excluding the quantum mechanical zero-point energy of the adsorbed hydrogen atom.

The energy for the single hydrogen E_H is $E_H^{GGA\text{-}II}=-13.639$ eV and $E_H^{LDA}=-13.034$ eV, respectively, for H in supercells of the size $5\times5\times5$ Å, using a plane-wave cutoff energy of 50 Ry and including spin effects. The GGA-II energy in the supercell is close to the energy obtained (-13.649 eV) using an atomic basis set.[21] The energies $E_{H,Ni}$ and E_{Ni} are evaluated using the present slab calculation. The final result is $E_{ads}^{GGA\text{-}II}=-2.76$ eV and $E_{ads}^{LDA}=-3.38$ eV using GGA-II and LDA, respectively.

Early first-principles calculations on the system were made by Weinert and Davenport[22] who used the spin polarized full-potential linear augmented-plane-wave method (FPLAPW), Umrigar and Wilkins[23] who used the nonspin

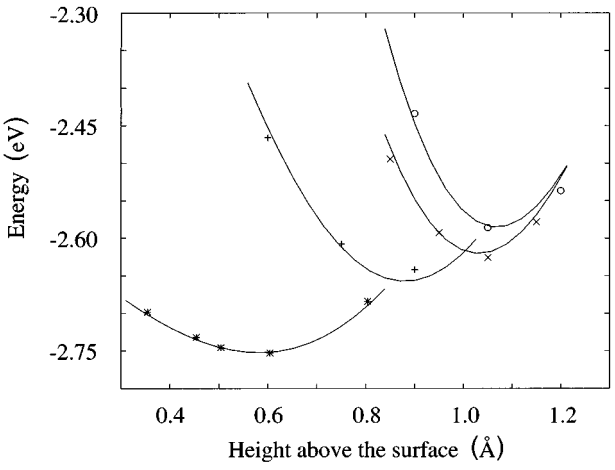

FIG. 2. The energy as a function of height above the surface: first-principles data (points) and the model potential (full line). *: hollow site (H) , +: mid site (M), ×: bridge site (B), and ○: off site (O). The model potential has, as can be seen in the figure, a slightly larger barrier (132 meV) than the first-principles data (127 meV).

TABLE I. H on Ni(001), experimental data and first-principles results for the adsorption energy, adsorption height, perpendicular frequency (harmonic approximation), and barrier height for diffusion (energy difference between the hollow and bridge sites excluding the change in zero-point energy).

	Energy (eV)	Height (Å)	$\hbar\omega_\perp$ (meV)	Barrier (meV)
Experimental data				
Stensgaard and Jakobsen (Ref. 27)		0.50 ± 0.10		
Lapujoulade and Neil (Ref. 25)	-2.8			
Christmann *et al.* (Ref. 26)	-2.8			
Karlsson *et al.* (Ref. 39)			78	
First-principles results				
Upton and Goddard (Ref. 24)	-3.04	0.30	73	310
Weinert and Davenport (Ref. 22)	-3.28[a]			
Umrigar and Wilkins (Ref. 23)	-3.42	0.32	90	80
Present work, LDA	-3.38	0.54	102	173
Present work, GGA-II	-2.76	0.57	100	127

[a]We have added the quantum mechanical zero-point energy.

polarized FPLAPW, and Upton and Goddard[24] who performed Hartree-Fock calculations on a Ni_{20} cluster. Results from these calculations are quoted in Table I and compared with experimental data and our calculations.

Our LDA result shows the expected overbinding but the GGA-II gives an adsorption energy which is in quantitative agreement with the available experimental results. The experimental data are from flash-desorption experiments by Lapujoulade and Neil[25] and Christmann, Schober, Ertl, and Neumann[26] which both were further analyzed by Wonchoba, Hu, and Truhlar[7] in order to find the adsorption energy.

Transmission channeling experiments, made by Stensgaard and Jakobsen,[27,28] measured the adsorption height and the data are in good agreement with our calculations. We find the equilibrium height to be 0.57 Å and the experimental value is 0.50 ± 0.10 Å.[27,28]

The vibrational frequencies given in Table I are in the harmonic approximation. In the next section we will determine the vibrational properties more accurately by solving the Schrödinger equation for the hydrogen atom and we postpone a discussion of these numbers to that section.

Umrigar and Wilkins[23] calculated the difference between hollow and bridge to be only 0.080 eV but since they used different muffin-tin radii at the hollow and bridge sites this value is questionable. The barrier height obtained by Upton and Goddard[24] differs a lot from the other data. Experimental values of the activation energy for diffusion are in the range 0.139–0.174 eV.[1,3,29,30] In Sec. V we will consider the zero-point motion effect on the activation energy and we can then make a more direct comparison with the experimental numbers.

III. MODEL POTENTIAL

The next step is to make use of the first-principles datapoints to derive a model potential for the hydrogen-metal interaction. For metallic systems a variety of simple many-atom potentials has been introduced to handle bonding in metals which all could be represented by the expression

$$E_{\rm tot}=\sum_i F_i(\rho_i)+\frac{1}{2}\sum_{i\neq j}\phi_{ij}(r_{ij}). \tag{2}$$

They have been named pair-functional methods[31] but the physical interpretation behind the functions in Eq. (2) differs among the different methods. In the effective medium theory (EMT) (Refs. 32,33) and the embedded atom method (EAM) (Ref. 11,34,35) the first term represents the embedding energy of an atom in the background electronic density ρ_i due to the surrounding atoms while the second term is a correction written as a pair potential. The EMT is a hierarchy of approximations[36] and only in the most approximate level does it reduce to Eq. (2). The aim with the EMT is to provide expressions to evaluate the different terms entering Eq. (2) while the EAM is more empirical in nature. We have found here that to get a good fit to the first-principles data both terms in Eq. (2) have to be adjusted in an empirical manner and in that respect we follow the EAM description quite closely.

In the present paper we have restricted ourselves to a rigid metal lattice and the H-H interaction is neglected. The total energy can then be written as

$$E_{\rm tot}=F_{\rm H}(\rho)+\sum_i\left[\phi(r_i)+F_{\rm Ni}(\rho_i)\right], \tag{3}$$

where the sum is over the nickel atoms, ρ_i is the the electron density at the metal atoms, and $F_{\rm Ni}$ is the embedding energy for nickel. We have to determine three different quantities: the electron density ρ from the metal atoms at the position of the hydrogen atom, the embedding energy $F_{\rm H}(\rho)$ for hydrogen as a function of the electron density ρ, and the pair interaction $\phi(r)$ between hydrogen and a metal atom separated by the distance r.

The first-principles results for the electron density from the metal atoms are shown in Fig. 3. We show the density at the hollow and bridge positions as functions of the distance from the surface. In the EAM the electron density is obtained from a superposition of spherically symmetric atomic Hartree-Fock densities. The number of $4s$ electrons n_s is

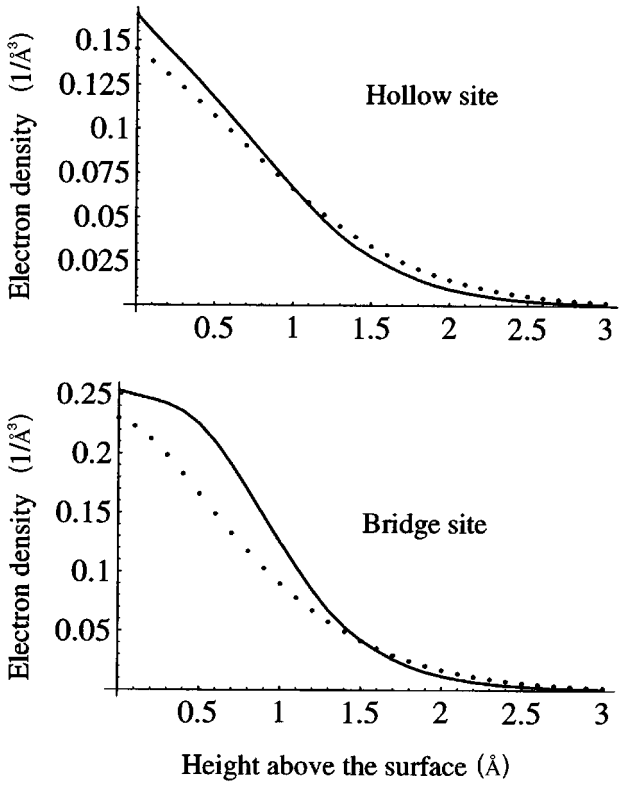

FIG. 3. Electron density as a function of height above the surface for the hollow site and the bridge site. The full lines are from the first-principles calculations and the dotted lines are from the EAM densities (superposition of atomic densities) with $n_s=2$. The density profile at the hollow site is well described by the atomic densities but the agreement is poorer for the bridge site. The position with lowest energy for hydrogen is at 0.6 Å above the surface at the hollow site and at 1.0 Å at the bridge site.

used as a fitting parameter and in previous studies the values $n_s=0.85$,[11] $n_s=1.52$,[34] and $n_s=2.0$ were used.[13,7,8] We find here that the value $n_s=2.0$ leads to the best agreement with the first-principles results (see Fig. 3). A slightly better agreement can be obtained using $n_s=2.2$, but the improvement is marginal and we have decided to use the value $n_s=2.0$. As can be seen in Fig. 3 the agreement at the hollow site is quite good while it is less satisfactory at the bridge site. Especially the gradient of the density fails at the bridge site. The charge is redistributed at the surface and the superposition of spherical atomic centered densities is questionable. We believe this to be the reason for the difficulties in transferability between different surfaces.[7] Wonchoba and Truhlar[8] have very recently tried to incorporate effects of the charge density gradient in order to achieve a more transferable potential.

For the embedding function $F_H(\rho)$ we first tried to use the embedding energy for H in an homogeneous electron gas determined using the density-functional theory together with the GGA-II approximation,[21] thereby reducing the fitting to the pair-interaction term. However, we found that to get a good agreement with the first-principles data the embedding function $F_H(\rho)$ also has to be included in the fitting procedure. We have used the following analytical form for the embedding energy:

$$F_{\mathrm{H}}(\rho)=\alpha_{\mathrm{H1}}\rho\exp[-\beta_{\mathrm{H1}}\rho]+\alpha_{\mathrm{H2}}\rho\exp[-\beta_{\mathrm{H2}}\rho], \quad (4)$$

TABLE II. Various parameters entering the expressions for the model potential. The seven parameters α_{H1}, β_{H1}, α_{H2}, β_{H2}, a_{H}, b_{H}, and c_{H} have been determined by fitting to the first-principles data points; d_{H} and e_{H} are introduced for numerical reasons only (see text). The parameters for Z_{Ni} are from Ref. 34.

$F_{\mathrm{H}}(r)$		
α_{H1}	306.371	eV Å^3
β_{H1}	5.8637	Å^3
α_{H2}	−373.783	eV Å^3
β_{H2}	6.5588	Å^3
$Z_{\mathrm{H}}(r)$		
a_{H}	0.15486	Å
b_{H}	0.29139	Å
c_{H}	4.7557	
d_{H}	0.15	Å
e_{H}	4.50	Å^{-2}
$Z_{\mathrm{Ni}}(r)$		
$Z_{0\mathrm{Ni}}$	37.9326	$\sqrt{\text{eV Å}}$
β_{Ni}	0.8957	Å^{-1}
α_{Ni}	1.8633	Å^{-1}
ν_{Ni}	1.0	

similar to the one used by Wonchoba and Truhlar[8]. The pair-interaction term is written in the usual form

$$\phi(r)=\frac{Z_{\mathrm{Ni}}(r)Z_{\mathrm{H}}(r)}{r} \quad (5)$$

with

$$Z_{\mathrm{Ni}}(r)=Z_{0\mathrm{Ni}}(1+\beta_{\mathrm{Ni}}r_{\mathrm{Ni}}^{\nu})\exp(-\alpha_{\mathrm{Ni}}r) \quad (6)$$

as in Ref. 34 and for $Z_{\mathrm{H}}(r)$ we have assumed the form

$$Z_{\mathrm{H}}(r)=\left(\frac{r}{b_{\mathrm{H}}}\right)^{c_{\mathrm{H}}}\exp\left[-\frac{r}{a_{\mathrm{H}}}\right]+d_{\mathrm{H}}\exp[-e_{\mathrm{H}}r^2]. \quad (7)$$

The second term is for numerical purposes, necessary only when $r\rightarrow 0$, and it has no influence on the properties at normal distances. We have investigated a number of other functional forms of the effective charge, sums of two or three exponentials, and a form similar to Z_{Ni}, but the form in Eq. (7) gave the best fit.

We have fitted the potential to our first-principles GGA-II data by calculating and minimizing the mean square deviation χ^2 between the first-principles energy points in Fig. 2 α_i^{ref} and the corresponding results obtained using the model potential α_i,

$$\chi^2=\sum_{i=1}^{15}\left(\frac{\alpha_i-\alpha_i^{\mathrm{ref}}}{\Delta\alpha_i}\right)^2. \quad (8)$$

The sum is over the 15 points in Fig. 2 and $\Delta\alpha_i$ are allowed deviations from the first-principles data. Here α_i^{ref} was calculated using the atomic basis set energy for hydrogen $E_{\mathrm{H}}=-13.649$ eV which cause a 0.01 eV difference between Fig. 2 and Table I. All parameters are given in Table II. As can be seen in Fig. 2 the resulting model potential gives a quite good interpolation between the fits to the first-principles data points.

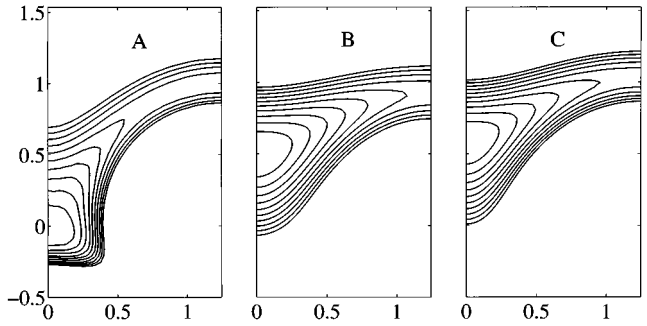

FIG. 4. The potential energy in a plane perpendicular to the (001) surface and through the hollow, mid, and bridge sites. A: the original EAM potential by Daw and Baskes (Ref. 11); B: the EAM parametrization used by Rice *et al.* (Ref. 13) and by Wonchoba *et al.* (Ref. 7); C: the current potential fitted to the first-principles calculations. Each energy contour differs by 25 meV and in all cases the energy at the hollow site is zero. The numbers on the axis are in Å.

In Fig. 4 we show two previously used model potentials, the original EAM by Daw and Baskes[11] and the EAM parametrization by Rice, Garret, Koszykowski, Foiles, and Daw,[13] together with our potential. Wonchoba, Hu, and Truhlar[7] have used a potential which is very similar to the one by Rice *et al.*[13] The differences are large between the original EAM potential and the later parametrizations. Significant effects on the dynamical properties are inevitable and comparisons between results obtained using different potentials[4,6,7] are very hard to make. The differences between the present potential and the parametrization by Rice *et al.*[13] and by Wonchoba *et al.*[7] are much smaller but not negligible: the barrier is lower, the vibrational frequencies perpendicular to the path are higher, and the adsorption height is slightly increased.

IV. VIBRATIONAL FREQUENCIES

The model potential will now be used to solve the three-dimensional Schrödinger equation for the hydrogen atom. Since the first-principles data cover the most important regions of the surface for hydrogen vibrations and tunneling we will mainly be interpolating between the first-principles data points when solving the Schrödinger equation. The metal host is kept frozen so no relaxations of the metal atoms are included.

The Hamiltonian was discretized using finite differences and a cubic mesh. The resulting matrix eigenvalue problem was solved using the Lanczos algorithm. This algorithm is very well suited to our problem because the lowest eigenvalues can be determined very accurately and efficiently.[37] The extent of the mesh in the x-y plane was chosen so that it contained exactly 1/4 of a periodic cell. By computing the ground-state energies for a set of k points (the Γ point and two points at the zone boundary X and M, using different boundary conditions at the cell boundaries,[38]) the bandwidth Δ was determined, defined as the difference in energy between the Γ and M points. Different grid spacings, down to 0.0311 Å, were used in order to control the discretization error. The values for the bandwidths were surprisingly stable when changing the grid spacing and the errors are less than

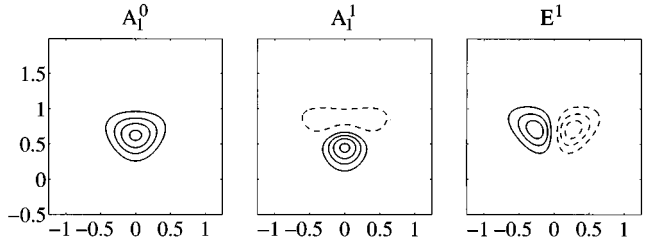

FIG. 5. The wave functions (for the Γ point) for the three lowest energy states for H on Ni(001) in a vertical plane along the $\langle 1\,\bar{1}\,0\rangle$ direction. The length of the cut is the surface lattice distance 2.49 Å and the cut is between two bridge sites. All contour lines are equally spaced and dashed lines correspond to negative numbers. The numbers on the axis are in Å.

3% for the ground-state bandwidth and less than 10% for the excited-state bandwidths. For the calculated excitation energies we find the discretization errors to be less than 2%.

In Fig. 5 we show the wave functions for the three lowest energy eigenstates. The A_1^1 state corresponds clearly to a vibrational excitation perpendicular to the surface while E^1 is parallel in character. The anharmonicity in the potential is seen in all wave functions. Higher excited states are of mixed parallel and perpendicular character. We identify the A_1^1 state with the prominent excitation seen in the high-resolution electron-energy-loss spectroscopy (HREELS) measurements[39] which differs from the identification made by Puska *et al.*,[40,38] who used a potential based on the effective medium theory (EMT). The reason is that the three-dimensional potential energy surfaces differ. The most important difference is that the EMT barrier is only of the order of 40–50 meV,[23] which gives a more pronounced parallel character of the A_1^1 state. The adsorption height (the maximum of the ground-state wave function) is also different. In the EMT potential it is 0.95 Å (Ref. 38) while in our case it is 0.57 Å.

We have performed calculations for both hydrogen and deuterium and the results are shown in Table III. The experimental values for the perpendicular and parallel excitations of hydrogen are 78 and 58 meV, respectively,[39,41] and for deuterium the corresponding values are 55 and 43 meV.[39,41] The perpendicular frequencies are measured at full coverage and for the (001) surface.[39] A direct comparison can be made and our numbers are found to be slightly too high, about 10%. The isotope shift is 1.39 compared with the experimental value 1.42. The parallel frequencies, however, are mea-

TABLE III. Energies and bandwidths for H/D on Ni(001).

	Hydrogen		Deuterium	
Band	Energy (eV)	Width (eV)	Energy (eV)	Width (eV)
A_1^0	0.121	22×10^{-9}	0.084	27×10^{-12}
A_1^1	0.207	12×10^{-6}	0.147	31×10^{-9}
E^1	0.189	3.6×10^{-6}	0.132	7.0×10^{-9}
	Excitation energy (meV)			
$\hbar\omega_\perp$	86		62	
$\hbar\omega_\parallel$	68		48	

sured more indirectly on the (510) surface[41] and some uncertainty is connected to the experimental numbers. For example, the perpendicular excitation for deuterium changes from 55 meV on the (001) surface[39] to 60 meV on (510).[41] We find again that our values are too high, with about 10%.

Our calculated bandwidths are much smaller than the bandwidths found by Puska and co-workers. For the A_1^1 state they find a bandwidth of 0.005 eV which is 400 times larger than ours. The reason again is the large difference in the potential. We notice that our results are more consistent with the spectroscopic data discussed in Ref. 42.

An important point is that the vibrational frequencies are lowered by 15% compared with the harmonic approximation (Table I). The harmonic approximation gives approximately 100 meV but the resulting value from the full calculation is 86 meV. Rick and Doll[43] have found a similar behavior for the vibrational states of H on Pd(111). This change in vibrational frequency makes it difficult to fit a model potential to experimental values for the frequencies.

The ground-state wave functions for deuterium can be compared with experimental results for the distribution from transmission channeling experiments by Stensgaard and Jakobsen. Our calculated spatial width $d=\sqrt{\langle x^2+y^2\rangle}$ (two-dimensional rms value) is $d=0.20$ Å and the experimental value is $d_{\rm exp}=0.20\pm0.04$ Å.[28]

V. TUNNELING MATRIX ELEMENTS

Our main interest is the diffusion process at low coverages. The measurements of the diffusion constant[1] do not show any strong coverage dependence neither for the activation energy and prefactor at high temperature nor for the tunneling diffusion constant at low temperature. It is not unreasonable to use the present model potential also for lower coverages, despite the fact that it is fitted to the first-principles data points for a monolayer. The HREELS measurements of the vibrational spectra[39] show that the hydrogen-hydrogen interaction can not be fully neglected but to a first approximation that is justified.

Adsorbate-adsorbate interaction is both direct and indirect.[44] The direct interactions are covalent bonding, Van der Waals interactions, and dipole-dipole interactions all of which are small at the present interatomic distance.[44] The indirect interaction (substrate mediated interaction) has two parts, an elastic interaction between the displacement fields of the adsorbed atoms and effects due to changes in the electronic structure at the surface. First-principles calculations performed at lower coverage will in the future be feasible and give a complete picture of the potential energy surface also for low coverage. The electronic contribution to the adsorbate-adsorbate interaction can then be calculated. The elastic interaction requires calculations on an even larger system, in the case of hydrogen it is in addition necessary to solve the Schrödinger equation and calculate the relaxations self-consistently. Recent calculations,[17] employing the present model potential show, however, that the relaxations are small and cannot solely account for the shift in vibrational energy observed experimentally.[39]

The bandwidth for hydrogen is extremely small and we expect the motion along the surface at low temperatures to be incoherent tunneling. Pertubation theory (golden rule) gives a simple estimate for the transition rate between two sites of the form

$$k=\frac{2\pi}{\hbar}J^2\rho, \tag{9}$$

where ρ is the density of final states and

$$J=\int d\mathbf{r}\Phi^*(\mathbf{r})\Delta U(\mathbf{r})\Phi(\mathbf{r}-\mathbf{R}) \tag{10}$$

is the tunneling matrix element between two localized states $\Phi(\mathbf{r}-\mathbf{R})$ and $\Phi^*(\mathbf{r})$ at neighboring sites separated by the distance $\mathbf{R}$. $\Delta U(\mathbf{r})$ is the difference from the local potential; added to the local potential it produces the full periodic potential.[45] $\Delta U(\mathbf{r})$ is thus a coupling between the localized states on neighboring sites and can be treated as a perturbation. For a square lattice the tracer diffusion constant is then given by $D=a^2k$ with $a=2.49$ Å for Ni(001). The potential is, as mentioned above, fitted to full-coverage data, which makes it only approximately correct for the low-coverage case.

The bandwidth Δ is directly related to the tunneling matrix element. In a tight-binding formulation of an s band assuming nearest-neighbor overlap only the energy is[45,46]

$$\epsilon(k)=\epsilon_0+\sum_{\rm NN}J\cos\mathbf{k}\cdot\mathbf{R}, \tag{11}$$

where $\mathbf{k}$ is the crystal momentum and the sum is over nearest-neighboring sites. The relation between the bandwidth, as defined in the previous section, and the tunneling matrix element is therefore $\Delta=8J$.

Experimentally one finds no pronounced isotope effect for diffusion at low temperatures.[1] The diffusion constant is found to be temperature independent for both H and D and the magnitude for both isotopes is similar. This is unexpected and not understood. One effect that influences the isotope dependence is the shape of the three-dimensional potential energy surface. If the region around the barrier top has higher curvature compared with the stable site the effective barrier for hydrogen will be larger compared with deuterium due to the two transverse degrees of freedom. We have here determined the bandwidth for both H and D. These two numbers differ by a factor 10^3 and we then expect, based on Eq. (9), that the diffusion constants will differ by about a factor 10^6. We conclude that the observed isotope effect at low temperatures cannot be explained by tunneling in a three-dimensional static potential.

To make it more explicit and quantify the importance of the three-dimensional potential we write the matrix element in the WKB approximation:

$$J=\left(\frac{\hbar\omega}{2\pi}\right)\exp\left[-\frac{1}{\hbar}\int_{-s_0}^{s_0}\sqrt{2m[V_{\rm mep}(s)-E]}ds\right]. \tag{12}$$

The turning points $\pm s_0$ are determined by the condition that $V_{\rm mep}(s=\pm s_0)=E$, where $V_{\rm mep}(s)$ is the potential along the minimum energy path, E is the ground-state energy, and ω is the vibrational frequency at the potential minimum. Assuming a single harmonic oscillator density of states $\rho=1/\hbar\omega$, we arrive at the following expression for the transition rate:

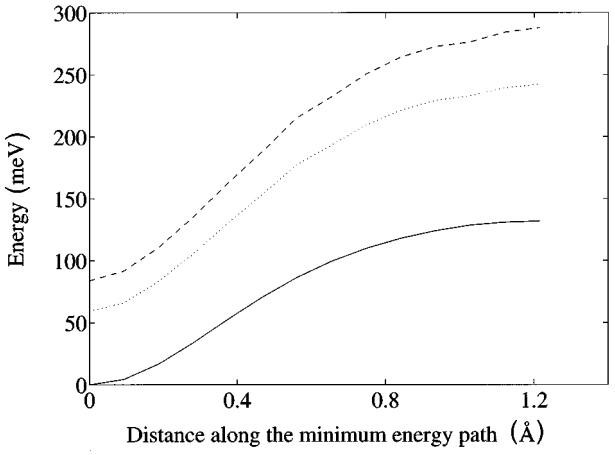

FIG. 6. The potential energy along the minimum energy path between the hollow site and the bridge site $V_{\mathrm{mep}}(s)$ (full line). The two other curves show the effective potentials for hydrogen $V_{\mathrm{eff}}^{\mathrm{H}}(s)$, (dashed line) and deuterium $V_{\mathrm{eff}}^{\mathrm{D}}(s)$ (dotted line) along the same path. The effective potentials contain the zero-point energy for the two transverse degrees of freedom.

$$k=\frac{\omega}{2\pi}\exp\left[-\frac{2}{\hbar}\int_{-s_0}^{s_0}\sqrt{2m[V_{\mathrm{mep}}(s)-E]}ds\right]. \qquad (13)$$

Eq. (12) assumes that the motion is one dimensional. To approximately account for the three-dimensional motion of the hydrogen atom one can add the zero-point energies for the two transversal degrees of freedom along the tunneling path.[47,10] $V_{\mathrm{mep}}(s)$ in Eq. (13) is then replaced by an effective isotope-dependent potential

$$V_{\mathrm{eff}}^{\mathrm{H}}(s)=V_{\mathrm{mep}}(s)+\frac{1}{2}\hbar\omega_1^{\mathrm{H}}(s)+\frac{1}{2}\hbar\omega_2^{\mathrm{H}}(s),$$

$$V_{\mathrm{eff}}^{\mathrm{D}}(s)=V_{\mathrm{mep}}(s)+\frac{1}{2}\hbar\omega_1^{\mathrm{D}}(s)+\frac{1}{2}\hbar\omega_2^{\mathrm{D}}(s), \qquad (14)$$

where $\omega_{1,2}^{\mathrm{H,D}}$ are the two frequencies along the minimum energy path for the two transversal degrees of freedom. The effective potentials, which are different for hydrogen and deuterium are shown in Fig. 6. The transversal modes are clearly important. The effective barrier heights are $\Delta_{\mathrm{eff}}^{\mathrm{H}}=204$ and $\Delta_{\mathrm{eff}}^{\mathrm{D}}=183$ meV for hydrogen and deuterium, respectively, which should be compared with the bare barrier height which for the model potential is equal to $\Delta_{\mathrm{bare}}=132$ meV (the 5 meV difference to the first-principles data in Table I is explained in Fig. 2). The WKB bandwidths for the *bare* potential are $\Delta_{\mathrm{bare}}^{\mathrm{H}}=670\times10^{-9}$ and $\Delta_{\mathrm{bare}}^{\mathrm{D}}=560\times10^{-12}$ eV compared with $\Delta_{\mathrm{eff}}^{\mathrm{H}}=6.6\times10^{-9}$ and $\Delta_{\mathrm{eff}}^{\mathrm{D}}=6.0\times10^{-12}$ eV using the effective potentials. The latter numbers are much closer to the bandwidths obtained by solving the Schrödinger equation numerically (see Table III).

The increase of the effective barrier for H compared with D is far too small to explain the absence of a pronounced isotope effect for diffusion at low temperatures. If we use the numerical values for the bandwidths obtained in the previous section together with Eq. (9) and $\rho=1/\hbar\omega$ we obtain $D^{\mathrm{H}}=6.6\times10^{-16}$ and $D^{\mathrm{D}}=1.4\times10^{-21}$ cm^2/s for the diffusion constant at low temperatures. The values are factors of 10^5 and 10^9 too small, respectively, compared with the experimental numbers. To explain the experimental isotope dependence the increase of the effective barrier has to be about twice as large for hydrogen as that for deuterium. Such a large effect should also give rise to a large difference in activation energy for diffusion around room temperature between the two isotopes. That is not observed. In contrary, the activation energy for deuterium seems to be slightly larger compared with hydrogen.[30]

We can now make a more detailed comparison with experiment for the barrier height. Also around room temperature the zero-point motion effect is important. To a first approximation the experimentally observed activation energy is equal to the effective barrier height minus the zero-point energy for one degree of freedom. We then obtain the results $\Delta E^{\mathrm{H}}=169$ and $\Delta E^{\mathrm{D}}=165$ meV for hydrogen and deuterium, respectively. We have also performed quantum Monte Carlo calculations of the diffusion constant using the path centroid formulation.[48] Around room temperature the diffusion constant is found to follow an Arrhenius behavior with the slope $\Delta E_{\mathrm{QMC}}^{\mathrm{H}}=167$ meV. This number is surprisingly close to the more crude estimate above. The corresponding experimental numbers are $\Delta E^{\mathrm{H}}=152\pm13$ and $\Delta E^{\mathrm{D}}=190\pm20$ meV, respectively. If we had used the results based on the LDA instead our barrier heights would have been about 50 meV higher (see Table I).

We can therefore conclude that the GGA-II for the exchange-correlation energy seems to reproduce the experimentally observed activation energy for hydrogen diffusion on the Ni (001) surface. The results using the LDA instead give an activation energy that is too high compared with experiments.

VI. SUMMARY AND CONCLUSIONS

We have performed electron-structure calculations for hydrogen adsorbed on the Ni (001) surface using the density-functional theory. Two different approximations for the exchange and correlation potential are used, the local-density approximation (LDA) and the generalized gradient approximation (GGA-II).[19] The LDA calculations are performed self-consistently, whereas the nonlocal corrections of the GGA-II are evaluated from the LDA densities. A slab configuration is used and we have restricted ourselves to one monolayer of hydrogen for computational reasons.

The calculated adsorption energy and binding distance are both found to be in excellent agreement with the experimental data.[25–28] For the former it is crucial to use the GGA-II to obtain an accurate number.

By fitting the limited number of first-principles data points to an analytical expression of EAM type we have also determined the hydrogen bandstructure by solving the Schrödinger equation for the hydrogen on a three-dimensional grid. An efficient numerical method based on the Lanczos algorithm is used[37] to calculate the eigenvectors and eigenvalues. The model potential, which is a result of the optimization procedure, is found to reproduce quite well the first-principles results and we are therefore essentially interpolating between the first-principles data points when solving the Schrödinger equation.

The vibrational frequencies for both H and D are found to

be slightly too high, with about 10%, compared with the experimental numbers.[39,41] For a proper evaluation of the vibrational frequencies a quantum-mechanical approach has to be used. Determining the perpendicular vibrational frequency from the curvature at the bottom of the well leads to a frequency 16% too high compared with the quantum mechanical solution. The width of the ground-state wave function for deuterium is also found to agree with experiments.[27,28]

We find that the barrier height for diffusion at high temperatures (above ~100 K) is in good agreement with experiments. Our potential has been derived for a monolayer of hydrogen but the experiments are performed at lower coverages. However, they do not show any strong coverage dependence neither for the activation energy nor for the prefactor.[1] The agreement is better if the GGA-II data are used compared with LDA. Similar conclusions have been drawn for hydrogen dissociation on metal surfaces.[49] A proper comparison has to include the so-called zero-point motion effect which is substantial also at room temperature.

We have also considered the experimentally observed absence of a pronounced isotope effect for diffusion at low temperatures (below ~100 K).[1,3] In the present paper we have determined the bandwidth of the ground state for both H and D with high accuracy. The bandwidth is directly related to the tunneling matrix elements for motion in a static three-dimensional potential. Even in absence of lattice motion unconventional isotope effects can be obtained due to the shape of the potential energy surface. If the curvature of the potential perpendicular to the tunneling path increases when moving from the center to the bridge position the isotope effect will be less pronounced compared with the usual squareroot dependence in the WKB exponent. We find here that the curvature at the bridge position is indeed larger compared with the equilibrium site, the center position, but the change is far too small to explain the experimental results.

To conclude, the present study shows that first-principles electron-structure calculations can now be used to determine with quite high accuracy the potential energy surface for hydrogen interacting with transition metal surfaces. This will be of crucial importance in the future in elucidating the mechanism for hydrogen diffusion on metal surfaces at low temperatures. This problem has very recently become even more important to investigate theoretically due to conflicting experimental results.[1,3,50,51]

ACKNOWLEDGMENTS

We would like to thank Ivan Stensgaard and Jan Hartford for useful discussions and providing us with their unpublished results. Financial support from the Swedish Natural Sciences Research Council (NFR), the Swedish Board for Industrial and Technical Development (NUTEK), and the Danish Research Councils through The Center for Surface Reactivity and Grant No. 9502053 as well as allocation of computer time at the Center for Parallel Computers (PDC) in Sweden is gratefully acknowledged. The Center for Atomic-Scale Materials Physics (CAMP) is sponsored by the Danish National Research Foundation.

*Electronic address: tfktm@fy.chalmers.se
†Electronic address: wahnstrom@fy.chalmers.se
‡Electronic address: tfylb@fy.chalmers.se
§Electronic address: hammer@fysik.dtu.dk

[1] T. S. Lin and R. Gomer, Surf. Sci. **255**, 41 (1991).
[2] X. D. Zhu, A. Lee, A. Wong, and U. Linke, Phys. Rev. Lett. **68**, 1862 (1992).
[3] A. Lee, X. D. Zhu, L. Deng, and U. Linke, Phys. Rev. B **46**, 15 472 (1992).
[4] T. R. Mattsson, U. Engberg, and G. Wahnström, Phys. Rev. Lett. **71**, 2615 (1993).
[5] L. Y. Chen and S. C. Ying, Phys. Rev. Lett. **73**, 700 (1994).
[6] T. R. Mattsson and G. Wahnström, Phys. Rev. B **51**, 1885 (1995).
[7] S. E. Wonchoba, W.-P. Hu, and D. G. Truhlar, Phys. Rev. B **51**, 9985 (1995).
[8] S. E. Wonchoba and D. G. Truhlar, Phys. Rev. B **53**, 11 222 (1996).
[9] K. A. Muttalib and J. Sethna, Phys. Rev. B **32**, 3462 (1985).
[10] A. Auerbach, K. F. Freed, and R. Gomer, J. Chem. Phys. **86**, 2356 (1987).
[11] M. S. Daw and M. I. Baskes, Phys. Rev. B **29**, 6443 (1984).
[12] S. M. Foiles, M. I. Baskes, C. F. Melius, and M. S. Daw, J. Less-Common Met. **130**, 465 (1987).
[13] B. M. Rice, B. C. Garret, M. L. Koszykowski, S. M. Foiles, and M. S. Daw, J. Chem. Phys. **92**, 775 (1990).
[14] J. K. Nørskov, J. Chem. Phys. **90**, 7461 (1989).
[15] M. C. Payne, M. P. Teter, D. C. Allan, T. A. Arias, and J. D. Joannopoulos, Rev. Mod. Phys. **64**, 1045 (1992).
[16] B. Hammer and J. K. Nørskov, Nature (London) **376**, 238 (1995).
[17] T. R. Mattsson and G. Wahnström (unpublished).
[18] N. Troullier and J. L. Martins, Phys. Rev. B **43**, 1993 (1991).
[19] J. P. Perdew, J. A. Chevary, S. H. Vosko, K. A. Jackson, M. R. Pederson, D. J. Singh, and C. Fiolhais, Phys. Rev. B **46**, 6671 (1992).
[20] L. Bengtsson (unpublished).
[21] U. Yxklinten, J. Hartford, and T. Holmquist, Phys. Scr. **55**, 449 (1997).
[22] M. Weinert and J. W. Davenport, Phys. Rev. Lett. **54**, 1547 (1985).
[23] C. Umrigar and J. W. Wilkins, Phys. Rev. Lett. **54**, 1551 (1985).
[24] T. H. Upton and W. A. Goddard III, Phys. Rev. Lett. **42**, 472 (1979).
[25] J. Lapujoulade and K. S. Neil, Surf. Sci. **35**, 288 (1973).
[26] K. Christmann, O. Schober, G. Ertl, and M. Neumann, J. Chem. Phys. **60**, 4528 (1974).
[27] I. Stensgaard and F. Jakobsen, Phys. Rev. Lett. **54**, 711 (1985).
[28] I. Stensgaard (unpublished).
[29] S. M. George, A. M. DeSantolo, and R. B. Hall, Surf. Sci. **159**, L425 (1985).
[30] D. R. Mullins, B. Roop, S. A. Costello, and J. M. White, Surf. Sci. **186**, 67 (1987).
[31] A. E. Carlsson, in *Solid State Physics*, Vol. 43 of *Solid State Physics*, edited by H. Ehrenrich and D. Turnbull (Academic Press, New York, 1990), p. 1.
[32] K. W. Jacobsen, J. K. Nørskov, and M. J. Puska, Phys. Rev. B **35**, 7423 (1987).
[33] K. W. Jacobsen, Comments Condens. Matter Phys. **14**, 129 (1988).

[34] S. M. Foiles, M. I. Baskes, and M. S. Daw, Phys. Rev. B **33**, 7983 (1986).
[35] M. S. Daw, S. M. Foiles, and M. I. Baskes, Mater. Sci. Rep. **9**, 251 (1993).
[36] N. Chetty, K. Stokbro, K. W. Jacobsen, and J. K. Nørskov, Phys. Rev. B **46**, 3798 (1992).
[37] L. Bengtsson, M.S. thesis, Chalmers University of Technology, 1993.
[38] M. J. Puska and R. M. Nieminen, Surf. Sci. **157**, 413 (1985).
[39] P. A. Karlsson, A. S. Mårtensson, S. Andersson, and P. Nordlander, Surf. Sci. **175**, L759 (1986).
[40] M. J. Puska, R. M. Nieminen, M. Manninen, B. Chakraborty, S. Holloway, and J. K. Nørskov, Phys. Rev. Lett. **51**, 1081 (1983).
[41] A.-S. Mårtensson, C. Nyberg, and S. Andersson, Surf. Sci. **205**, 12 (1988).
[42] R. R. Cavanagh, J. J. Rush, and R. D. Kelley, Phys. Rev. Lett. **52**, 2100 (1984).
[43] S. W. Rick and J. Doll, Surf. Sci. **302**, L305 (1994).
[44] P. Nordlander and S. Holmström, Surf. Sci. **159**, 443 (1995).
[45] N. W. Ashcroft and N. D. Mermin, *Solid State Physics* (Saunders College, Philadelphia, 1976).
[46] W. A. Harrison, *Solid State Theory* (McGraw-Hill, New York, 1970).
[47] A. Auerbach and S. Kivelson, Nucl. Phys. B **257** [FS14], 799 (1985).
[48] T. R. Mattsson and G. Wahnström, in *Surface Diffusion: Atomistic and Collective Processes*, NATO Advanced Studies Institute, Series B: edited by M. Tringides (Plenum, New York, in press).
[49] B. Hammer, M. Scheffler, K. W. Jacobsen, and J. K. Nørskov, Phys. Rev. Lett. **73**, 1400 (1994).
[50] G. X. Cao, A. Wong, and X. D. Zhu, Bull. Am. Phys. Soc. **41**, 421 (1996).
[51] G. X. Cao and X. D. Zhu, in *Surface Diffusion: Atomistic and Collective Processes* (Ref. 48).